Axial and radial segregation of granular mixtures in a rotating spherical container

Lama Naji and Ralf Stannarius
Institute of Experimental Physics, Otto von Guericke University, Universitätsplatz 2, D-39106 Magdeburg, Germany
(Received 8 January 2009; revised manuscript received 3 March 2009; published 27 March 2009)

We report the formation of axial segregation patterns of bidisperse granular mixtures of glass beads in a spherical container which is rotated about a central axis. When the rotation axis is horizontal, three distinct segregation bands are formed for a broad range of geometrical and dynamical parameters. We find two distinct regimes: at low fill levels the small size beads of the mixture are collected at the poles and the large size beads in a central band. At high fill levels the pole regions are occupied by large beads, while the small beads form the central band. The critical fill level for this structural transition decreases with increasing container size. For a container with 37 mm inner diameter, containing a mixture of 0.5 and 1.5 mm beads, the transition occurs between 40% and 50% fill level. When the rotation axis is tilted, the band positions are shifted and two-band structures are formed with the smaller particles at the lower pole. In our experiments the granulate is submersed in water; this allows NMR imaging of the complete three-dimensional band structures. We compare the observed segregation structures to those in cylindrical mixers and propose a model for the qualitative explanation of the pattern formation process.

DOI: 10.1103/PhysRevE.79.031307 PACS number(s): 45.70.Mg, 45.70.Qj, 05.65.+b, 83.85.Fg

I. INTRODUCTION

Agitated granular mixtures can reveal a number of counterintuitive phenomena [1–4], for example, their size and density segregation under various conditions. These phenomena have been known for many decades. Oyama [5] started pioneering work already in 1939. Many experiments with granular materials such as spherical glass beads, salt, sand, seeds, and pharmaceutical pills have been performed since that time, and computer simulations have been reported, but the physical origins of some of the observed phenomena are still not understood very well.

Particles may differ in size, density, or both size and density. Rotating mixers of cylindrical, rectangular, and spherical geometries have been used [5–32]. Surface flow in tumblers of different geometries is discussed in a recent paper by Meier *et al.* [33]. We restrict ourselves in this work to the description of slowly rotating mixers (no ballistic particle motion) and focus on the phenomena in bidisperse mixtures (by size) of glass beads, which are often representative for the structures and effects found in other material combinations.

It is known that the segregation in a long cylindrical or rectangular mixer proceeds in three phases. First, after a few rotations, the material segregates radially [6]. The smaller beads form a core enclosed by the larger beads. This segregation process is quite well understood. The second phase is an axial instability of the core [16,19,20]. This instability is not always present; it depends upon the rotation speed of the mixer and upon particle properties. The granulate can develop an axial band structure after several hundred rotations of the mixer. The third phase is a coarsening of this band structure [15], which ends when the granular material is completely demixed into two or three bands. It has been shown experimentally [7] that these scenarios are found in mixers of different cross section shapes, and that similar patterns can be observed in dry granulate as well as in slurries (granulate completely submersed in a liquid of lower density, e.g., [7,8,25,30,31]). Arndt *et al.* [8] have presented a study of the influence of different filling levels on the segregation process in long cylindrical mixers. We will compare their results to analogous experiments performed here with a spherical mixer.

Apart from studies of very short [practically two-dimensional (2D)] drums, experimental investigations have been focused so far mainly to mixers with large aspect ratio, i.e., with axial extensions large compared to their diameter. The influences of the lateral boundaries on the segregation pattern period can often be neglected in these situations (but see, for example, [7,17]). However, technical applications often involve short compact mixers, e.g., in pharmaceutical applications [34]. Some results have been reported also for short cylindrical and for spherical containers. Chen *et al.* [35] studied the velocity fields and influences of lateral container walls in short cylinders and quasi-2D mixers numerically. Zik *et al.* [11] reported experiments in cylindrical mixers with a lateral modulation of the radius. These cylinders have bottlenecks (small radius segments) in which the larger particles accumulate, while the smaller particles of the mixture collect in the segments of large radius. These experiments indicate that the radius variation has direct influence on segregation. A few investigations of more complex mixer geometries such as double cones [36] or v-shaped blenders [37] have been published. A complete three-dimensional (3D) analysis of segregation patterns was reported by Kawaguchi *et al.* [38]. In their experiments, proton magnetic resonance imaging (MRI) of capsules in a conical short cylinder was employed. Gilchrist and Ottino [39] investigated spherical mixers under the combined influence of rocking and rotation by means of optical methods. This work motivated the present study of a rotating spherical container with optical and NMR methods.

We fill spherical containers with a granular mixture and rotate them about a central axis. The small aspect ratio and the container side walls play a crucial role for the developing segregation structures.

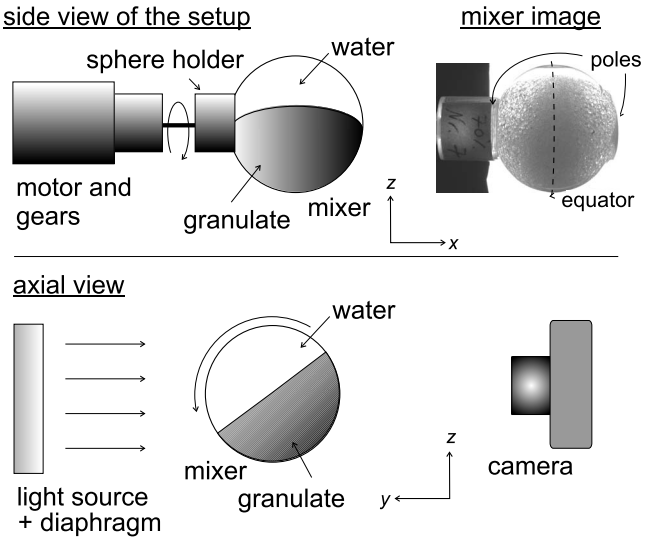

FIG. 1. Sketches of the experimental setup consisting of the mixer, a gear motor, light source, and camera. The sphere rotates such that upper part moves toward the light source. The camera takes pictures in transmission. The upper right image shows a 37 mm diameter sphere with 70% filling, after segregation at 10 rpm. The dark equatorial band consists of small beads, the brighter polar regions of large beads.

We use glass containers and observe the granulate optically in transmitted light. The segregated bands of large and small transparent glass beads can be clearly distinguished in transmission. In order to access the complete three-dimensional structure of the segregation patterns, additional experiments are performed with proton MRI. This method exploits the fact that our granular beads are embedded in water. The NMR image maps the water distribution in the spherical container and thus reveals the distribution of the individual beads in the mixer [30]. Finally, we investigate the influence of a tilt of the rotation axis on the formation of segregation bands and on the dynamics of the segregation patterns.

II. EXPERIMENT

The mixers consist of spherical glass containers of diameters between 3 and 3.7 cm. In addition, a 7 cm diameter plastic sphere is used in one experiment. If not stated otherwise, the data refer to 3.7 cm diameter glass spheres.

Figure 1 sketches the experimental setup together with typical image of a container filled with granulate, after segregation. A lateral holder is glued to the outer side of the sphere and connects it to a dc motor with gears. The rotation speed of the sphere can be varied between ≈ 2 and 30 rpm (rotations per minute). In this range, the Froude number $\mathrm{Fr} = R\omega^2/g$, given by the angular velocity ω of the sphere, the gravitational acceleration g, and the container radius R, is of the order of 10^{-3}. The Froude number is a measure for the ratio of inertial and gravitational forces on the grains.

The granulate is a bidisperse 50:50% by weight mixture of transparent glass beads. The smaller beads have diameters in the range from 0.5 to 0.63 mm. The diameter of the larger beads is in the range from 1.4 to 1.6 mm.

The sphere is illuminated by a diffuse light source, and transmission images are recorded with a Nikon Coolpix 4500 digital camera, computer controlled by software (KRINNICAM). The digital images are taken and stored automatically at regular intervals (usually 1 min). For image analysis we use the commercial software package IDL. A typical experiment covers between 100 and 10 000 revolutions of the sphere.

The two sides of the spherical container are geometrically identical. The containers are filled through a small opening of a few millimeters diameter on one side. After the container is filled with the granulate and water, the opening is sealed with epoxy glue. As a consequence, one side is glass and the opposite side contains a small spot of epoxy glue near the pole of the rotation axis. The experiments show that this detail is not relevant; the granulate on both sides behaves identically. In the images shown below, the glued right-hand side can be recognized by some excess epoxy outside the glass spheres.

Different filling levels of the spheres with granulate, between 20% and 90%, were achieved by weighing the granulate before filling the sphere. A 50% sample in our notation is a sphere which is half filled with granulate, so that the total volume fraction of the glass beads is around 30% of the container volume.

In addition to the spherical container, we have performed experiments with a short cylinder. This allows us to analyze the influences of lateral glass walls separately. This cylinder has a diameter to length ratio of 1:1; its inner diameter is 3.7 cm, equal to that of the medium-sized spherical mixers.

NMR experiments were performed with a Bruker BioSpec 47/20 MRI scanner operating at 200 MHz proton resonance frequency (4.7 T). We obtained optimal results with the RARE (rapid acquisition with relaxation enhancement) spin echo sequence. Water appears bright in the NMR images and the glass beads appear dark. The segregation structures were prepared outside the MRI magnet. Before scanning, the sphere was decoupled from the motor and inserted horizontally into the receiver coil with an opening of about 70 mm. The spatial resolution of the MRI experiment was better than the diameter of the small beads in the mixture, thus, individual glass beads can be resolved. On insertion of the sphere into the MRI scanner we took special care to keep the axis in horizontal position, but the rotation angle was not exactly preserved. We were not interested to obtain information on the angle of repose from the MRI experiments, although this is in principle possible when the rotation experiment is performed directly in the MRI scanner. From the complete 3D images, we selected here two types of representative slices defined in Fig. 2. The slice thickness is approximately equal to the size of the small beads, 0.5 mm.

III. RESULTS

A. Horizontal rotation axis, stationary structures

The first set of experiments was performed with spheres that are rotated with their axes horizontal. As is seen in Fig.

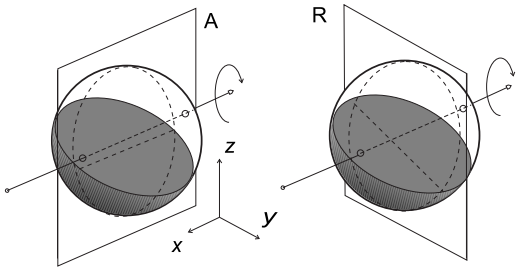

FIG. 2. Geometry of the slices presented from the NMR 3D imaging experiments. The axial slice (A) is a plane containing the rotation axis, whereas the radial slices (R) are normal to the rotation axis. Radial slices shown exemplarily in Figs. 4 and 5 are taken at different positions along the rotation axis.

3, a qualitative difference of the emerging segregation structures is found in dependence upon the filling level. The rotation speed in these examples was 10 rpm. At low filling level (below 40%), the granulate in the 37 mm spheres always develops three segregation bands after a few (10 to 20) rotations. A central (equatorial) stripe of large beads is flanked by two regions containing exclusively small beads near the poles of the rotation axis (we will denote this structure in the following by the abbreviation SLS for small-large-small). The complete 3D structure of this segregation pattern has been extracted by means of NMR imaging of the water in the container. Figure 4 below shows an axial slice (vertical cross section containing the rotation axis) and four representative radial slices (cross sections normal to the rotation axis, cf. Fig. 2). One can see that the central band of large beads contains a core structure of small beads connecting the two polar regions. This feature will become important later for the stripe dynamics at tilted rotation axes. The degree of segregation is very high; the polar regions are practically free of large beads.

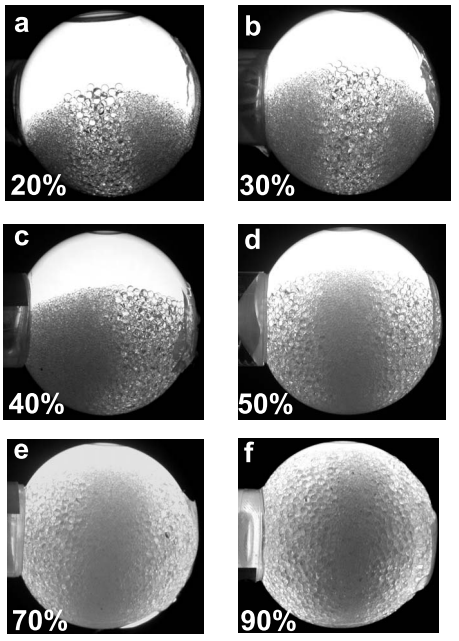

FIG. 3. Segregation patterns in a spherical mixer (diameter 37 mm) with filling levels from 20% (top left) to 90% (bottom right). In the optical images [(a) and (b)], at filling levels below 40%, one can distinguish a segregation band of large beads in the equatorial plane and the two polar regions containing small beads. The patterns develop after only 5–10 rotations of the mixer and their structure remains stable and unchanged even after 10 000 rotations. Around 40% filling, different types of stable structures can develop, for example two-stripe patterns as shown in (c). At higher fill levels, optical images (d–f), a central segregation band of small beads is flanked by two polar regions containing large beads. All experiments were performed with a 50:50 wt.% mixture of large glass beads (≈1.5 mm diameter) with small beads (≈0.55 mm diameter).

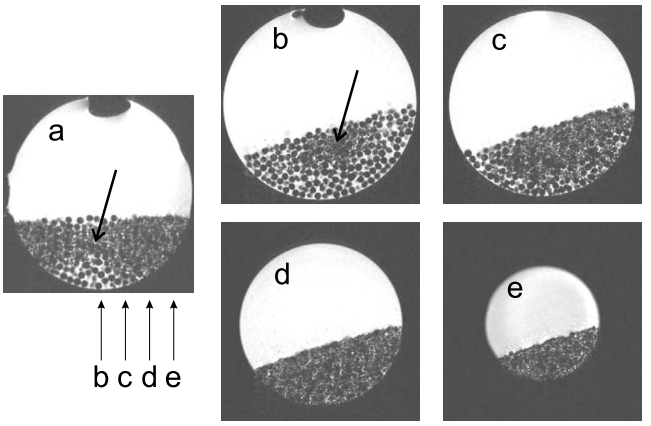

FIG. 4. Slices extracted from the 3D NMR image of a 30% filled container. The orientation of the axial slice (a) and radial slices (b–e) are defined in Fig. 2. Vertical arrows mark the positions of the radial slices (b–e), taken in 5 mm steps starting at the equator. The complete NMR data provide 0.5 mm resolution. We present every 10th slice here and restrict ourselves to one side of the equator for symmetry reasons. Arrows in slices (a) and (b) point at the core of small beads.

An opposite structure is found in containers with high filling levels (50% and above), as shown in Figs. 3(d)–3(f). Here, the central region contains exclusively small beads, while the large size component of the granular mixture collects in the polar regions. We will refer to this structure by the abbreviation LSL (large-small-large). Again, the segregation is almost perfect. The NMR images (Fig. 5) show that the polar regions are now practically free of small beads, and the central equatorial region is almost completely formed by small beads. The small size beads form some rudimentary core structure into the neighboring regions of large beads [Figs. 5(d) and 5(e)]. The two polar regions of large beads are almost completely separated from each other.

If the filling level is around 40%, the situation is not clearly determined. Often, SLS type patterns are found between 40% and 50% fill level, sometimes LSL type patterns are found near 40% filling, and occasionally stable two-stripe patterns form [Fig. 3(c)]. Sometimes a very slow dynamics was observed. Within the typical duration of experiments (less than 10 000 rotations) no clear trend toward a general preferential state was discernible in this transition range.

The formation of the structures is not very sensitive to the rotation speed. Segregation was observed already at rotation rates of 2 rpm. At such low rates, the final quality of segre-

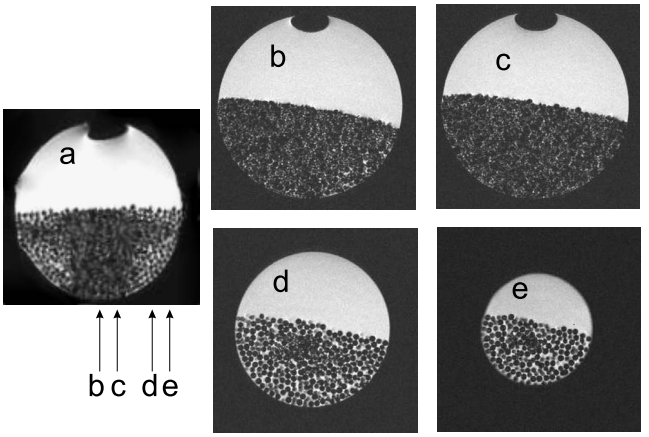

FIG. 5. Slices extracted from the 3D NMR image of a 50% filled container. The axial slice (a) is oriented as shown in Fig. 2. Vertical arrows mark the positions of the radial slices (b–e).

gation was not as excellent as at faster rotation rates (at the same number of revolutions). When the rotation speed is 5 rpm and higher, well segregated stripes are formed. The fastest rotation rate in our experiments was 30 rpm, where still excellent segregation structures were formed.

Experiments with larger and smaller container sizes showed qualitatively similar results. However, in the small containers (30 mm diameter) a higher rotation rate was necessary to obtain the three-band structures. As a general tendency we have found that in the large containers (70 mm) the LSL structure is stable at lower filling rates than in the 37 mm spheres, they could be observed occasionally even at 30% filling fraction. In the smaller containers, the SLS structure seems to be more stable, but very often the granulate spontaneously formed two-band (LS or SL) structures. Figure 6 shows two representative images of a 30 mm sphere which develops SLS patterns even at 50% fill level, but somewhat faster rotation rates, and of a 70 mm sphere which developed LSL patterns even at 30% fill level. Note that the two images in Fig. 6 do not have the same scale.

In order to understand the influences of different geometrical factors on the pattern formation process, we performed two additional experiments. First, we studied a cylindrical container with the same width to diameter ratio as the spheres. The purpose of this experiment is to understand

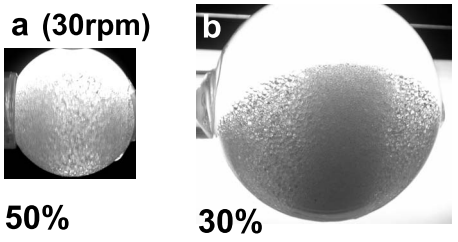

FIG. 6. In smaller containers, the transition from SLS to LSL patterns shifts to higher filling fractions, whereas in larger containers, the SLS to LSL transition is found at lower filling fractions. The optical images show SLS patterns in a 30 mm diameter sphere (a) at 50% filling level, and LSL patterns in a 70 mm diameter sphere (b) at 30% fill level.

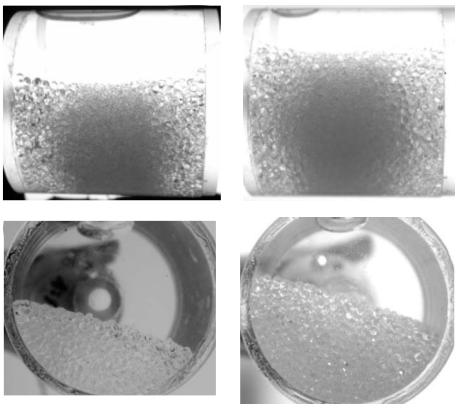

FIG. 7. Segregation patterns in a cylindrical mixer of 37 mm diameter, filling levels are 30% (left column) and 50% (right column). Optical images at the top show the view perpendicular to the rotation axis, as in the sphere experiment. The dark stripe represents the band of small beads. The corresponding pictures in the bottom row are taken in direction of the axis. They demonstrate that exclusively large beads collect at the end wall.

whether a lateral wall supports the preferential aggregation of small beads or of large beads (possible influences of friction on segregation) or whether this lateral wall is neutral with respect to the two species. Figure 7 shows the clear result: the lateral glass walls lead to a formation of boundary layers of large beads, and the cylinders develop three-band LSL structures *independent* of the fill level. This feature will be discussed in the final section in the context of the fill-level dependence of the structures found in the spherical mixers.

One has to be careful to generalize the observations in glass bead mixtures. For example, Kawaguchi *et al.* [38] found different behavior in mixtures of polystyrene and gelatine spheres in cylindrical acrylic drums. These authors report a slight trend toward an increased concentration of large particles at the sides, but the radial core always extends to the cylinder ends. Moreover, this trend is reversed in certain mixtures in a conical drum.

A further set of experiments has been performed to test the influence of sieve effects. It is well known from experiments in shaken containers that smaller particles accumulate at the bottom of a container filled with an initially uniform mixture, while the larger particles accumulate at the top of the granular layer (Brazil nut effect). In the case of the horizontal cylindrical mixer, the rotation forces the smaller grains from falling all the way to the bottom, resulting in a core of small particles. Thus the sieve effect contributes to radial segregation, but it does not play a role in redistributions along the cylinder axis. In the spherical mixer, however, one has to consider that the granular layer is deeper in the central (equatorial) region. This may lead to a preferential aggregation of the small-size component near the equatorial zone. An appropriate experiment to test this hypothesis and to demonstrate the sieve effect is the tilt of the rotation axis.

B. Oblique rotation axis, dynamics of stripes

First, we discuss experiments with containers of low filling ratio that develop LSL patterns when they are rotated

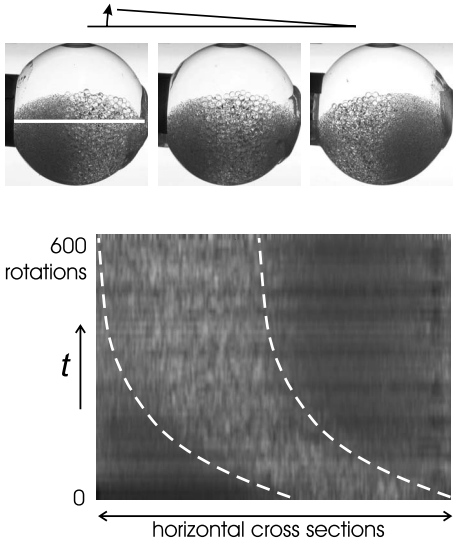

FIG. 8. Pattern dynamics at tilted rotation axes, 37 mm container at 30% filling, 10 rpm: We start with a two-stripe SL pattern (left image). The axis tilt is 4°, see arrow, this causes a continuous shift of the central band of large beads toward the higher pole. The middle image was taken after 60 rotations, the right-hand image after 560 rotations. The space-time plot at the bottom has been constructed from horizontal slices taken at the position of the white line in the upper left picture. The larger beads appear brighter in this space-time plot. Dashed lines mark the approximate borders of the bands of small and large beads.

about a horizontal axis. When the rotation axis is tilted, the three-band structure rapidly transforms into a two-band structure. The small beads in the upper polar region migrate through the central band of large beads into the bottom region. The initial structure in the first image of Fig. 8 has been created by tilting the rotation axis of the sphere by −6° to the left (not shown here). Within about 200 rotations, the small beads gathered in the lower (left) and the large beads collected in the upper (right) hemisphere as shown in the left image of Fig. 8. After that, the axis tilt has been changed to 4° to the right (see top of Fig. 8).

Figure 8 shows that this LS structure is reversed when the rotation axis is tilted in the opposite direction. A tilt of just a few degrees is sufficient for the exchange of the stripes. The space-time plot at the bottom of Fig. 8 has been assembled from 60 sequential images taken in 60 s steps. Central horizontal cross sections of these images (white bar in the top left picture) have been stacked, time runs from bottom to top. The final stationary pattern consists of two well-separated bands of small and large beads, where the small beads are located in the lower half sphere. In a similar way, any initial SLS segregation structure or completely mixed granulate transforms into the two-band structure when the rotation axis deviates from the horizontal by a few degrees.

This effect is symmetric and not caused by slight asymmetries of the container itself (see remark about the filling technique). When the tilt is reversed, the corresponding space-time-plot is practically a mirror image of that in Fig. 8.

Figure 9 shows NMR images of a 50% filled sample with 37 mm diameter which has been rotated about a tilted axis. The central slice shown in Fig. 9(b) is practically free of

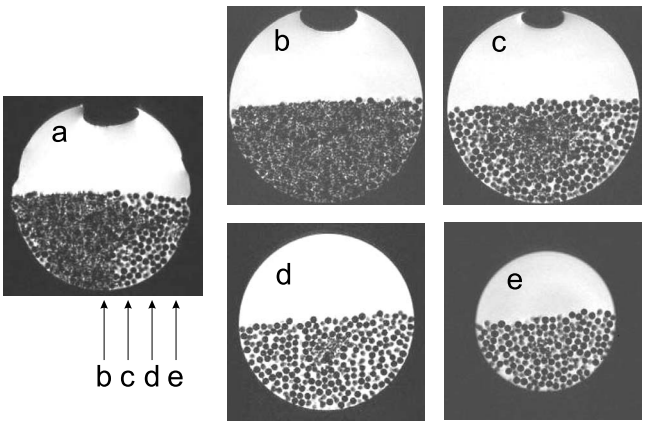

FIG. 9. Slices of the 3D NMR image of a 50% filled container with slightly tilted rotation axis. The sample was inserted in the MRI scanner with the free surface turned into horizontal orientation. Slice (a) contains the rotation axis. The vertical arrows indicate the positions of the radial slices (b–e), taken in 5 mm steps starting at the equator.

large beads; only a few large beads are found on the top. On the other hand, the small size beads form only some very rudimentary core structure into the neighboring region of large beads [Fig. 9(c)]. In contrast to Fig. 5, the segregation pattern in Fig. 9(a) is not symmetric; the left-hand stripe of large beads is almost missing, because the axis of rotation was tilted during segregation (right-hand side up).

When the same experiment is performed with large fill levels, the situation is different. The central band of an LSL structure is rather stable, at least at small tilt angles. The central stripe may shift slightly to one side but the two polar regions of large beads do not vanish, except at very large tilt angles 20° and above) and high rotation speeds (20 rpm and above). In this case, one can also observe the motion of the small beads toward the lower pole (Fig. 10). Again, this resulting two-band pattern can be reversed when the tilt direction is reversed. If the tilt of the axis is around 10° or lower, or if the rotation speed is 10 rpm and lower, then there is no observable dynamics of any segregated band structures within the time range of our experiments, no matter whether the initial patterns consist of two or three bands.

The explanation of the difference with the SLS dynamics in containers with low filling level is obvious. The central band of large beads of the SLS structure in the latter contains

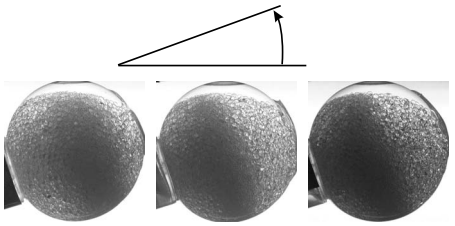

FIG. 10. Shift of the LSL pattern in a container with 70% filling ratio. The initial LSL bands were obtained by rotating the sample about a horizontal axis. The first image was taken immediately after the 20° tilt of the rotation axis. The second and third images were recorded after 3380 and 10,660 rotations, respectively

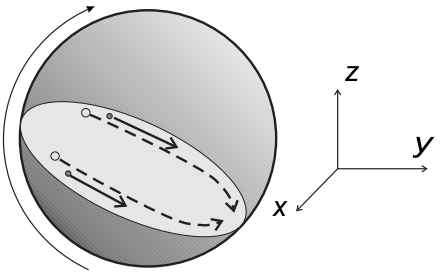

FIG. 11. Schematic picture of the supposed motion of small and large beads in the fluidized bed inside the spherical container. The small sized beads slide along the gradient and come to a rest before they reach the opposite container walls (solid paths), while the large beads slide to the end of the slope and are then forced away from the poles by the container walls (dashed paths).

an inner core of small particles [Figs. 4(a) and 4(b)], which serves as an exchange channel between the two polar bands. In the containers with large filling ratio, the central band of small beads in an LSL structure does not contain large beads [cf. Figs. 5(a)–5(c)]. These beads cannot pass the small bead stripe. A similar observation has been made in cylindrical containers earlier [30,31]. Thus, exchange between the polar regions of large beads through the central band is inhibited, and any exchange dynamics is slower by orders of magnitude.

IV. DISCUSSION

On the basis of the observations described in the previous section, we interpret the observed effects and develop the following model:

In spherical containers with different filling ratios, at least three competing mechanisms control the formation, positions, and dynamics of segregation bands. As is clear from the short cylinder experiments, where large beads are found in the outer stripes and small beads collect in the center of the mixer, the lateral glass walls support the collection of large particles (I). This is presumably related to differences in friction. If the region near the lateral wall consists mainly of large particles, there are less contact points of the granulate with the walls of the container. This friction is known to influence the dynamics of granulate at the cylinder ends [40,41]. It is, however, not evident how this friction might be related to the observed accumulation of large beads at the end walls. If we transfer the observation made in cylinders to the spherical geometry, it is obvious that spheres with filling ratios of 50% and above will develop a preference for LSL structures. In spheres with low filling ratios, this effect is less effective since the regions near the poles are not occupied by granulate.

A competing mechanism that should be particularly effective in containers with lower filling level is sketched in Fig. 11 (II).

As is well established, e.g., for cylindrical mixers but also for other free surfaces of granular mixtures, larger beads slide over longer distances on the free surface of a granular bed, while the smaller grains are often trapped before they reach the mixer walls. In the spherical container, the small grains near the poles that slide on the surface will essentially stay in that region. They come to rest before they reach the end of the slope. The large beads, after reaching the end of the free surface plane, encounter the container walls. The end of the inclined plane of the fluidized bed is curved in the sphere container. Thus, the large beads that reach the container walls will be forced toward the equator of the sphere. We suggest that this effect supports SLS pattern formation in particular at low and intermediate fill levels. For filling levels much above 50 %, the axis is submersed below the free surface of the granulate. Material directly at the poles does not reach the free surface at any time, therefore the effect becomes less important. We would also like to note that this mechanism gets weaker in general for larger containers (where the corresponding radius of curvature is larger). This may qualitatively explain the shift of the LSL to SLS transition with container size (cf. Fig. 6).

Very likely, a third effect has to be considered in the spherical container as well (III). As we have shown in the tilted axis experiments, the small beads have a tendency to move to the bottom of the container. This sieve effect is similar to the Brazil nut effect found in shaken containers. Since small beads in a mixed region often find holes to fall into lower regions, they tend to collect toward the bottom of the rotating spheres. In a cylindrical mixer, the rotation of the container brings them continuously up again, so that a radially segregated core is formed. In a rotating sphere with oblique axis, there is a component of the gravitational force along the rotation axis which is sufficient for an axial drift of the material and gradual collection of the small particles near the lower pole. Experiments with tilted rotating cylinders were performed by Arndt *et al.* [8]. The axial drift of the small grains toward the lower pole of the rotation axis is similar in both situations.

Now we apply this idea to the spheres with nontilted rotation axes. If the axis is horizontal, there is no gravitationally preferred pole region, but the granular layer is deeper in the central region of the sphere. Therefore the smaller particles would like to go away from the poles. A concentration of small beads in the equatorial region will be preferred by a mechanism similar to the Brazil nut effect. The difference of depth of the granular layer in the equatorial and outer regions is small in shallow beds, i.e., at low fill ratios. There, other effects may dominate this one. Thus the tendency for small beads to collect in the equatorial regions will increase with larger filling level. It seems that this kind of Brazil nut effect is the same that provides segregation mechanism in cylinders of modulated radii [11].

Combining the proposed segregation mechanisms, we find that the first and last of the three effects (I-III) favor the formation of LSL structures in spherical mixers of high filling level. Effect (II), sketched in Fig. 11, supports the formation of SLS type segregation structures. Together, these competing influences on the granulate may be responsible for the observed types of segregation patterns and for the structural transition with increasing fill level of the mixer. A crude sketch of the relevance of the three mechanisms is shown in Fig. 12.

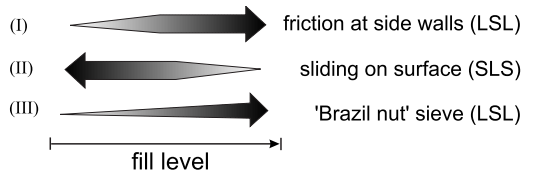

FIG. 12. Sketch of the three suggested segregation mechanisms and their effectiveness in dependence upon the fill level of the spherical mixer.

V. SUMMARY

It has been shown by optical and MRI experiments that different axial segregation structures are formed by granular mixtures in rotating spherical containers. When a spherical drum filled with a bidisperse mixture of glass beads is rotated about its horizontal axis, a structural transition in dependence upon the fill level of the mixer is observed. At low fill levels, the small particles accumulate in the polar regions (SLS pattern). An axial core embedded in the band of large beads connects these polar regions of small beads. At high fill levels, the large particles are collected in the polar regions (LSL pattern). Segregation of the mixtures is almost complete. Only a rudimentary core of small beads extends from the central band into the adjacent regions of large beads. The critical fill level for the transition depends upon the ratio of container size to granular bead sizes.

Our model for a qualitative description of the observed pattern formation considers three competing segregation mechanisms. In dependence upon the container fill level, the efficiencies of these mechanisms vary. This leads to a selection of either LSL or SLS patterns. The model explains the basic features of our experimental observations.

A tilt of the rotation axis by a few degrees has dramatic consequences for the SLS structures. Within a few hundred rotations, the small beads accumulate at the lower pole, creating a two-stripe pattern. This structure can be reversed by reversal of the axis tilt. On the other hand, LSL structures are stable against a small tilt of the rotation axis. Only at large tilt angles and sufficiently high rotation speeds, LSL structures can be transformed into two-stripe patterns with the small beads at the lower pole.

After preparation of this paper, we have learned that similar patterns have been observed for dry granular mixtures in the same spherical mixer geometry by Chen *et al.* [42]. Their data obtained for mixtures of different sizes in a container of given diameter agree qualitatively with our findings for a given mixture in containers of different sizes. The transition from LSL to SLS shifts in the same way with the ratio of mixer to grain dimensions. In addition to the experiments, numerical simulations are presented by these authors.

ACKNOWLEDGMENTS

We are indebted to Thomas John, Tilo Finger, and Frank Rietz for interesting discussions, and particularly to Thomas John for technical support. Frank Angenstein, Jörg Stadler, and the Leibniz Institute for Neurobiology Magdeburg are acknowledged for providing the technical basis and support in the MRI experiments. The authors are much indebted to J. M. Ottino for making manuscript [42] available prior to publication.

[1] G. H. Ristow, *Pattern Formation in Granular Material* (Springer, Berlin, 2000).
[2] L. P. Kadanoff, Rev. Mod. Phys. **71**, 435 (1999).
[3] H. M. Jaeger, S. R. Nagel, and R. P. Behringer, Rev. Mod. Phys. **68**, 1259 (1996).
[4] J. M. Ottino and D. V. Khakhar, Annu. Rev. Fluid Mech. **32**, 55 (2000).
[5] Y. Oyama, Sci. Pap. Inst. Phys. Chem. Res. (Jpn.) **6**, 600 (1939); **37**, 17 (1940).
[6] E. Clément, J. Rajchenbach, and J. Duran, Europhys Lett. **30**, 7 (1995); F. Cantelaube and D. Bideau, *ibid.* **30**, 133 (1995).
[7] S. J. Fiedor and J. M. Ottino, Phys. Rev. Lett. **91**, 244301 (2003).
[8] T. Arndt, T. Siegmann-Hegerfeld, S. J. Fiedor, J. M. Ottino, and R. M. Lueptow, Phys. Rev. E **71**, 011306 (2005).
[9] M. B. Donald and B. Roseman, Br. Chem. Eng. **7**, 749 (1962).
[10] S. das Gupta, D. V. Khakhar, and S. K. Batia, Chem. Eng. Sci. **46**, 1513 (1991).
[11] O. Zik, D. Levine, S. G. Lipson, S. Shtrikman, and J. Stavans, Phys. Rev. Lett. **73**, 644 (1994).
[12] Z. S. Khan, W. A. Tokaruk, and S. W. Morris, Europhys. Lett. **66**, 212 (2004).
[13] V. Frette and J. Stavans, Phys. Rev. E **56**, 6981 (1997).
[14] M. Nakagawa, S. A. Altobelli, C. Caprihan, E. Fukushima, and E.-K. Jeong, Exp. Fluids **16**, 54 (1993).
[15] M. Nakagawa, Chem. Eng. Sci. **49**, 2540 (1994).
[16] M. Nakagawa, S. A. Altobelli, C. Caprihan, and E. Fukushima, Chem. Eng. Sci. **52**, 4423 (1997).
[17] K. M. Hill and J. Kakalios, Phys. Rev. E **49**, R3610 (1994).
[18] K. M. Hill and J. Kakalios, Phys. Rev. E **52**, 4393 (1995).
[19] K. M. Hill, A. Caprihan, and J. Kakalios, Phys. Rev. Lett. **78**, 50 (1997).
[20] K. M. Hill, A. Caprihan, and J. Kakalios, Phys. Rev. E **56**, 4386 (1997).
[21] K. M. Hill, D. V. Khakhar, J. F. Gilchrist, J. J. McCarthy, and J. M. Ottino, Proc. Natl. Acad. Sci. U.S.A. **96**, 11701 (1999).
[22] K. M. Hill, N. Jain, and J. M. Ottino, Phys. Rev. E **64**, 011302 (2001).
[23] K. Choo, T. C. A. Molteno, and S. W. Morris, Phys. Rev. Lett. **79**, 2975 (1997).
[24] K. Choo, M. W. Baker, T. C. A. Molteno, and S. W. Morris, Phys. Rev. E **58**, 6115 (1998).
[25] N. Jain, D. V. Khakhar, R. M. Lueptow, and J. M. Ottino, Phys. Rev. Lett. **86**, 3771 (2001).
[26] Z. S. Khan and S. W. Morris, Phys. Rev. Lett. **94**, 048002 (2005).
[27] A. Alexander, F. J. Muzzio, and T. Shinbrot, Granul. Matter **5**, 171 (2004).

[28] L. Prigozhin and H. Kalman, Phys. Rev. E **57**, 2073 (1998).
[29] S. J. Fiedor, P. Umbanhowar, and J. M. Ottino, Phys. Rev. E **73**, 041303 (2006).
[30] T. Finger, A. Voigt, J. Stadler, H. G. Niessen, L. Naji, and R. Stannarius, Phys. Rev. E **74**, 031312 (2006).
[31] T. Finger and R. Stannarius, Phys. Rev. E **75**, 031308 (2007).
[32] G. Juarez, J. M. Ottino, and R. M. Lueptow, Phys. Rev. E **78**, 031306 (2008).
[33] S. W. Meier, R. M. Lueptow, and J. M. Ottino, Adv. Phys. **56**, 757 (2007).
[34] S. Massol-Chaudeur, H. Berthiaux, and J. A. Dodds, Chem. Eng. Sci. **57**, 4053 (2002).
[35] P. Chen, J. M. Ottino, and R. M. Lueptow, Phys. Rev. E **78**, 021303 (2008).
[36] A. Alexander, T. Shinbrot, and F. J. Muzzio, Phys. Fluids **13**, 578 (2001).
[37] A. Alexander, F. J. Muzzio, and T. Shinbrot, Chem. Eng. Sci. **58**, 487 (2003).
[38] T. Kawaguchi, K. Tsutsumi, and Y. Tsuji, Part. Part. Syst. Charact. **23**, 266 (2006).
[39] J. F. Gilchrist and J. M. Ottino, Phys. Rev. E **68**, 061303 (2003).
[40] J. E. Maneval, K. M. Hill, B. E. Smith, A. Caprihan, and E. Fukushima, Granul. Matter **7**, 199 (2005).
[41] G. Metcalfe, L. Graham, J. Zhou, and K. Liffman, Chaos **9**, 581 (1999).
[42] P. Chen, B. J. Lochman, J. M. Ottino, and R. M. Lueptow, Phys. Rev. Lett. (to be published).